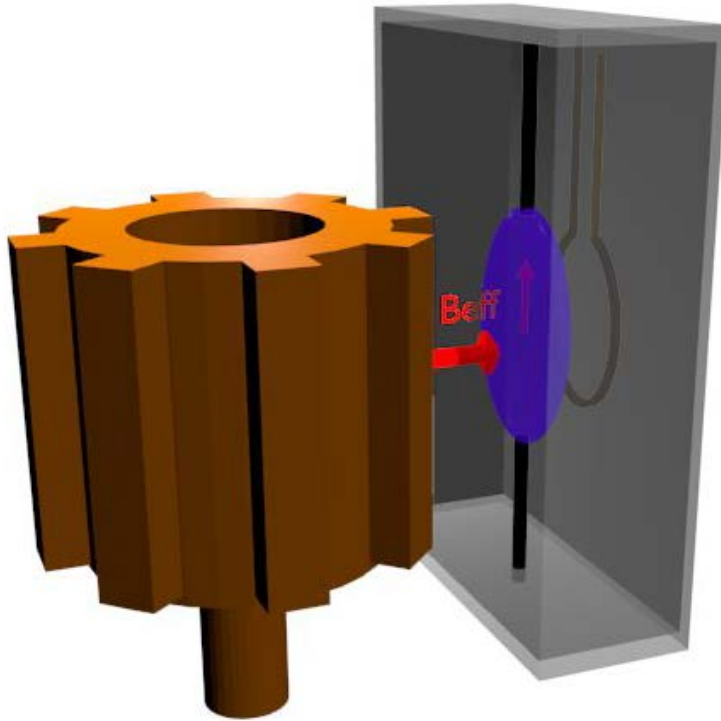


The Axion Resonant InterAction Detection Experiment (ARIADNE)



A. Geraci, University of Nevada, Reno

Tabletop experiments with skyscraper reach

Aug 9, 2017

Mark Cunningham (UNR)
Mindy Harkness (UNR)
Jordan Dargert (UNR)
Chloe Lohmeyer (UNR)
Harry Fosbinder-Elkins (UNR)
Asimina Arvanitaki (Perimeter)
Aharon Kapitulnik (Stanford)
Eli Levenson-Falk (Stanford)
Sam Mumford (Stanford)
Josh Long (IU)
Chen-Yu Liu (IU)
Mike Snow (IU)
Erick Smith (IU)
Justin Shortino (IU)
Inbum Lee (IU)
Evan Weisman (IU)
Yannis Semertzidis (CAPP)
Yun Shin (CAPP)
Yong-Ho Lee (KRISS)



iBS Institute for Basic Science

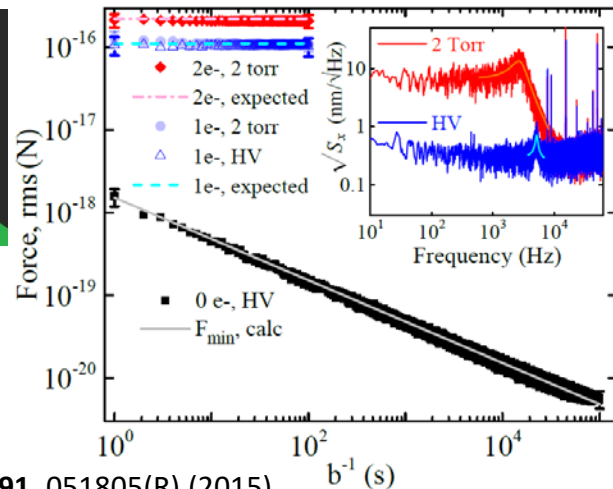
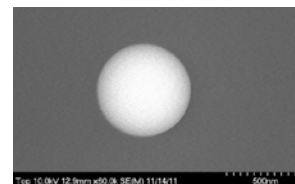
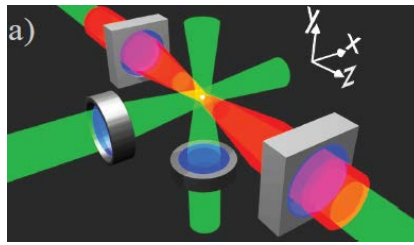
University of Nevada, Reno



Our lab: Fundamental physics with resonant sensors

Techniques

Mechanical Resonance: Optically levitated nanospheres



G. Ranjit et.al., *Phys. Rev. A* **91**, 051805(R) (2015).

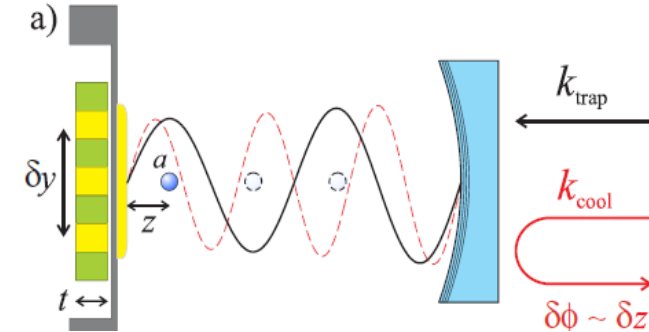
G. Ranjit, M. Cunningham, K. Casey, and AG, *Phys. Rev. A*, **93**, 053801 (2016).

Spin Resonance: NMR –Laser polarized gases or liquids



New Physics

Gravity at micron scales



AG., S. Papp, and J. Kitching, *Phys. Rev. Lett.* **105**, 101101 (2010).

Gravitational Waves

A. Arvanitaki and AG., *Phys. Rev. Lett.* **110**, 071105 (2013).

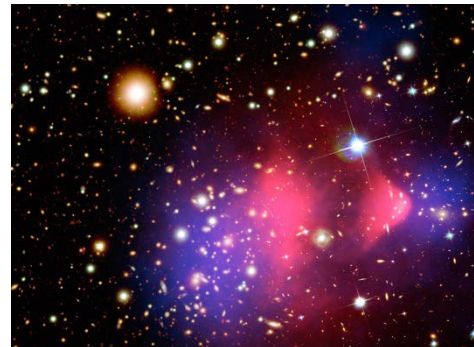
Spin-dependent forces • QCD Axion

A. Arvanitaki and AG., *Phys. Rev. Lett.* **113**, 161801 (2014).

Axions

- Light pseudoscalar particles in many theories Beyond Standard model
- Peccei-Quinn Axion (QCD) solves strong CP problem $\theta_{QCD} < 10^{-10}$
- Dark matter candidate

Experiments: e.g. ADMX, CAST, LC circuit, Casper



- R. D. Peccei and H. R. Quinn, Phys. Rev. Lett. 38, 1440 (1977);
- S. Weinberg, Phys. Rev. Lett. 40, 223 (1978);
- F. Wilczek, Phys. Rev. Lett. 40, 279 (1978).
- J. E. Moody and F. Wilczek, Phys. Rev. D 30, 130 (1984).

Axion couplings

$$\frac{a}{f_a} F_{\mu\nu} \tilde{F}^{\mu\nu}$$



Coupling to electromagnetic field
ADMX, DM Radio, LC Circuit (DM)
CAST, IAXO (solar)
ALPS, ALPS-II (light thru walls)

$$\frac{a}{f_a} G_{\mu\nu} \tilde{G}^{\mu\nu}$$

Coupling to gluon field

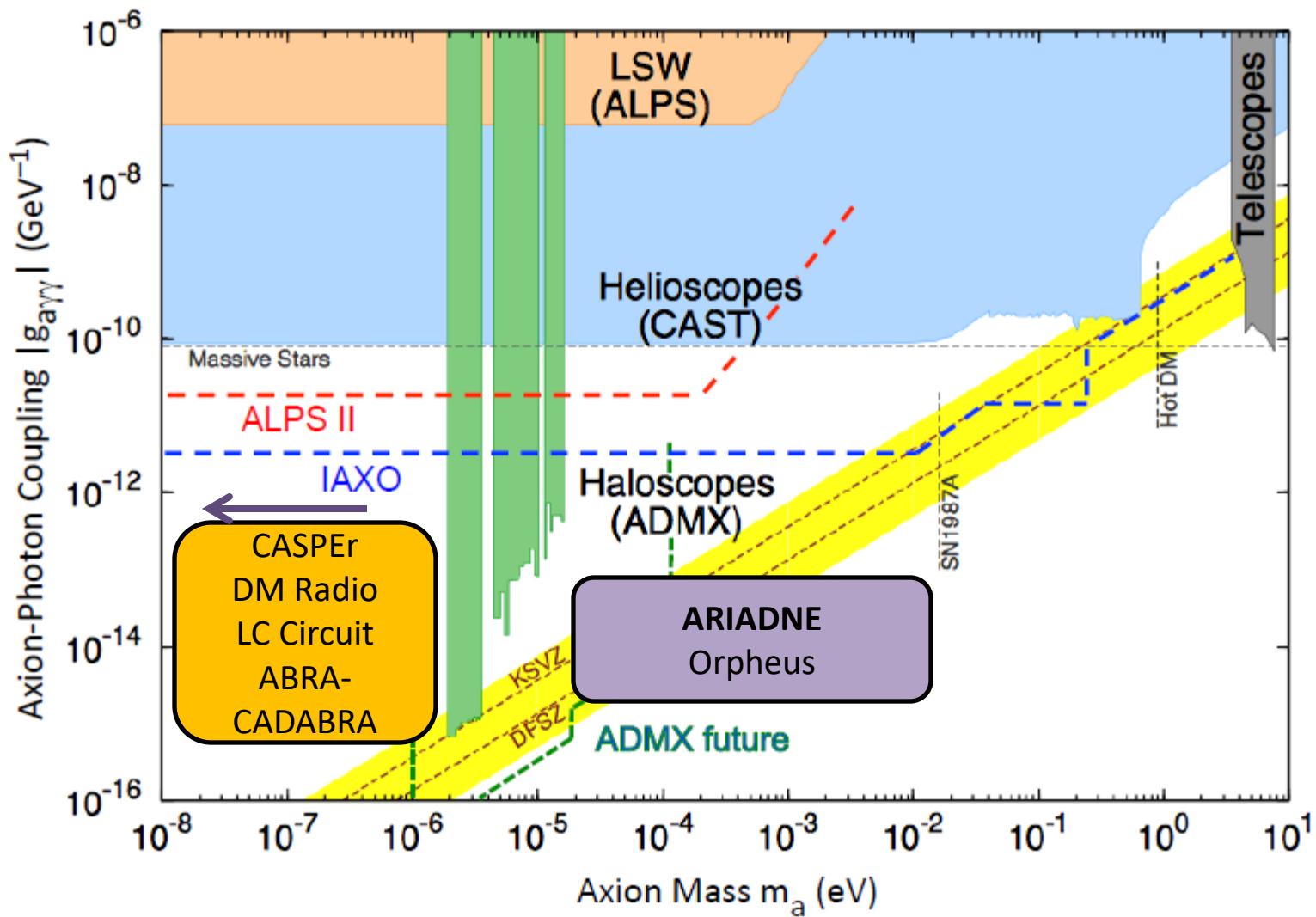
e.g. CASPER-electric (DM)

$$\frac{\partial_\mu a}{f_a} \bar{\Psi}_f \gamma^\mu \gamma_5 \Psi_f$$

Coupling to fermions

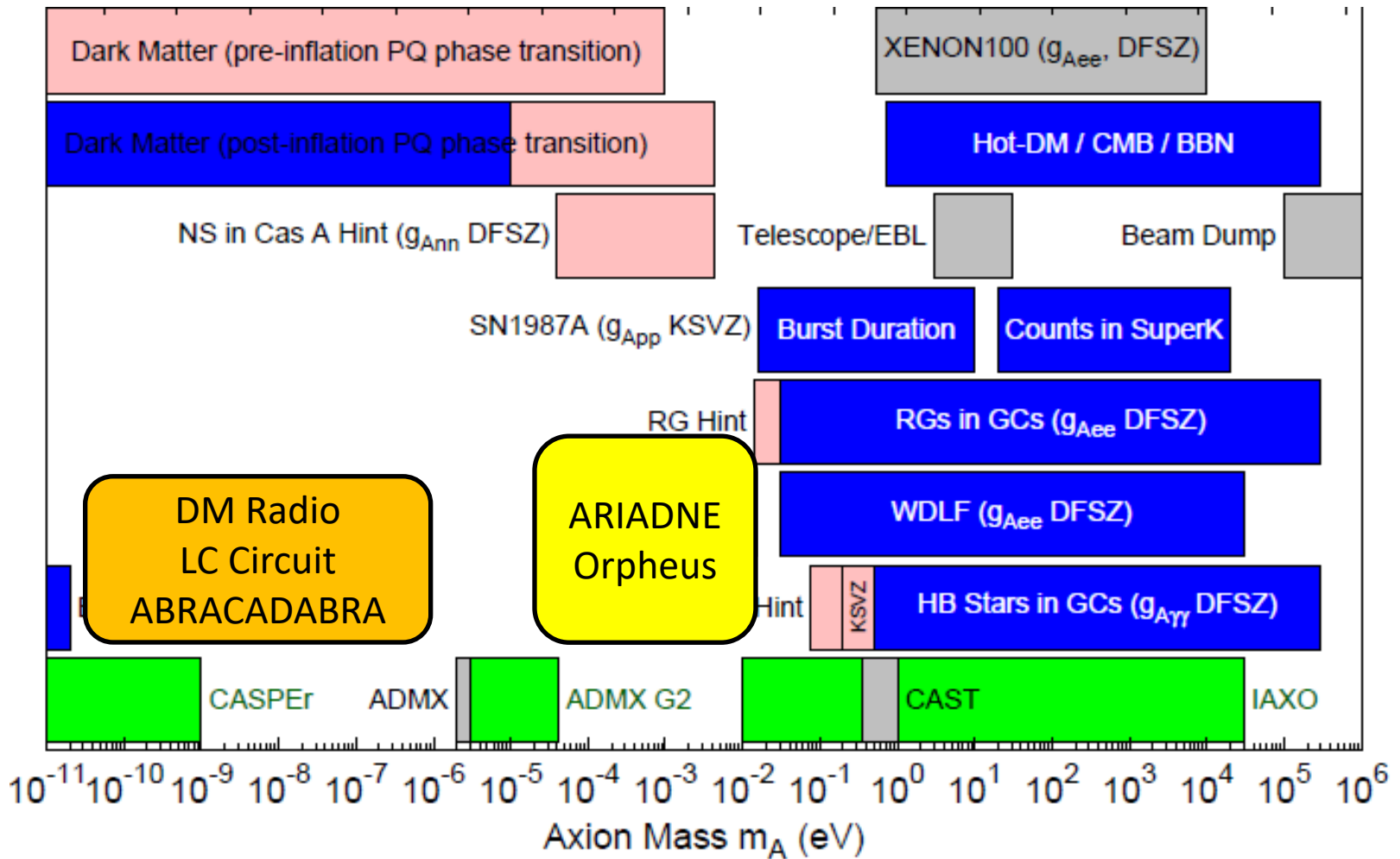
e.g. CASPER-wind, QUAX (DM)

Axion Parameter space



Adapted from Graham, arxiv: 1602.00039

QCD Axion parameter space



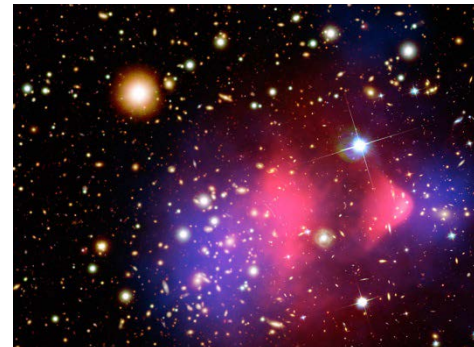
Axion and ALP searches

Source	Coupling	
Photons	Nucleons	
Dark Matter (Cosmic) axions	ADMX, ADMX-HF DM Radio, ABRA- CADABRA, LC Circuit, Orpheus	CASPER-Electric CASPER-Wind
Solar axions	CAST IAXO	
Lab-produced axions	Light-shining-thru- walls (ALPS, ALPS-II)	ARIADNE

Axions

- Light pseudoscalar particles in many theories Beyond Standard model
- Peccei-Quinn Axion (QCD) solves strong CP problem $\theta_{QCD} < 10^{-10}$
- Dark matter candidate

Experiments: e.g. ADMX, CAST, LC circuit, Casper



- Also mediates spin-dependent forces between matter objects at short range (down to 30 μm)

→ Can be sourced locally

- R. D. Peccei and H. R. Quinn, Phys. Rev. Lett. 38, 1440 (1977);
- S. Weinberg, Phys. Rev. Lett. 40, 223 (1978);
- F. Wilczek, Phys. Rev. Lett. 40, 279 (1978).
- J. E. Moody and F. Wilczek, Phys. Rev. D 30, 130 (1984).

Axion-exchange between nucleons

- Scalar coupling $\propto \theta_{\text{QCD}}$

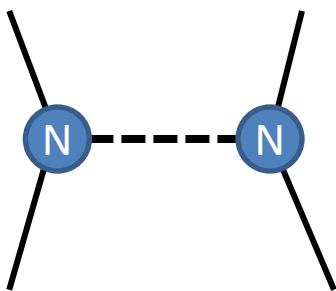
$$\mathcal{L} \supset \frac{\theta_{\text{QCD}}}{f_a} \mu a \bar{\psi} \psi$$

- Pseudoscalar coupling

In the non-relativistic limit:

$$\mathcal{L} \supset \frac{\vec{\nabla} a}{f_a} \cdot \vec{\sigma}$$

Axion acts a force mediator between nucleons



$$(g_s^N)^2$$

Monopole-monopole

A diagram showing a blue circular node labeled 'N' connected by a dashed line to a red oval. The oval represents an axion field.

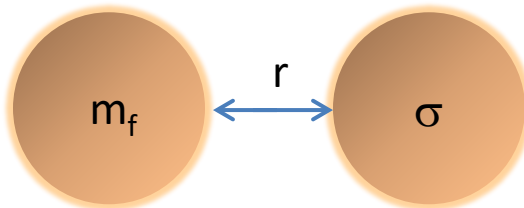
$$g_s^N g_P^N$$

Monopole-dipole

$$(g_p^N)^2$$

dipole-dipole

Spin-dependent forces



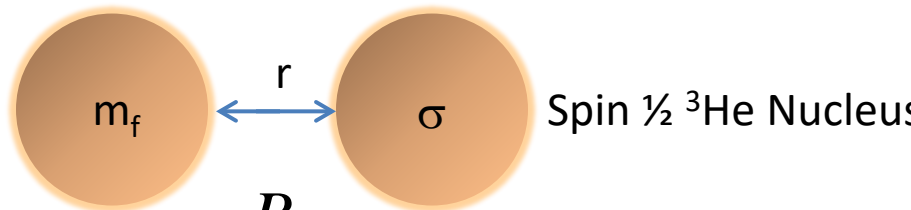
Monopole-Dipole axion exchange

$$U(r) = \frac{\hbar^2 g_s^N g_p^N}{8\pi m_f} \left(\frac{1}{r\lambda_a} + \frac{1}{r^2} \right) e^{-r/\lambda_a} (\hat{\sigma} \cdot \hat{r}) \equiv \mu \cdot B_{\text{eff}}$$

Fictitious magnetic field

- Different than ordinary B field
- Does not couple to angular momentum
- Unaffected by magnetic shielding

Using NMR for detection



$$U = \mu \cdot B_{\text{ext}}$$

Bloch Equations

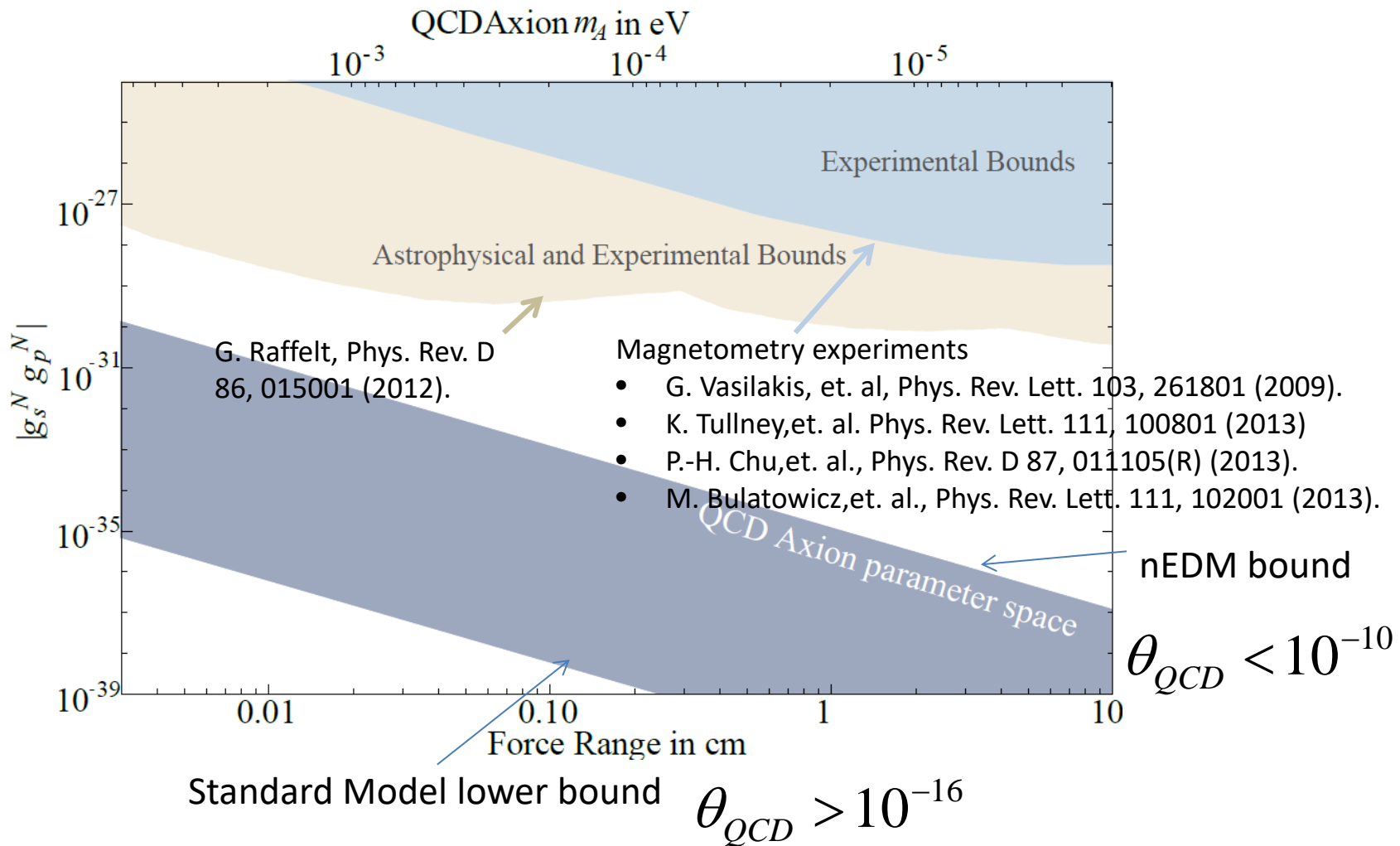
$$\frac{d\vec{M}}{dt} = \gamma \vec{M} \times \vec{B}$$

An energy level diagram for a spin $\frac{1}{2}$ system. Two horizontal blue lines represent energy levels. Above the top line is the state $|\uparrow\rangle$. Below the bottom line is the state $|\downarrow\rangle$. To the right of the lines, the equation $\omega = \frac{2\mu_N \cdot B_{\text{ext}}}{\hbar}$ is written.

Spin precesses at nuclear spin Larmor frequency $\omega = \gamma B$

Axion B_{eff} modifies measured Larmor frequency

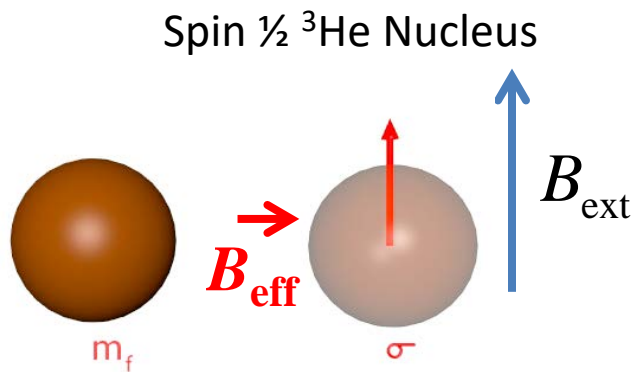
Constraints on spin dependent forces



ARIADNE: uses resonant enhancement

Oscillate the mass at Larmor frequency

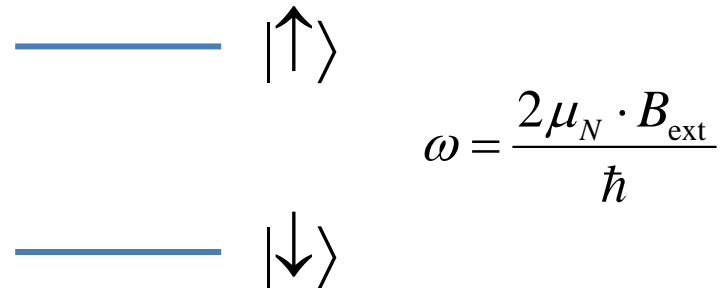
$$B_{\text{eff}} = B_{\perp} \cos(\omega t)$$



$$U = \mu \cdot B_{\text{ext}}$$

Bloch Equations

$$\frac{d\vec{M}}{dt} = \gamma \vec{M} \times \vec{B}$$



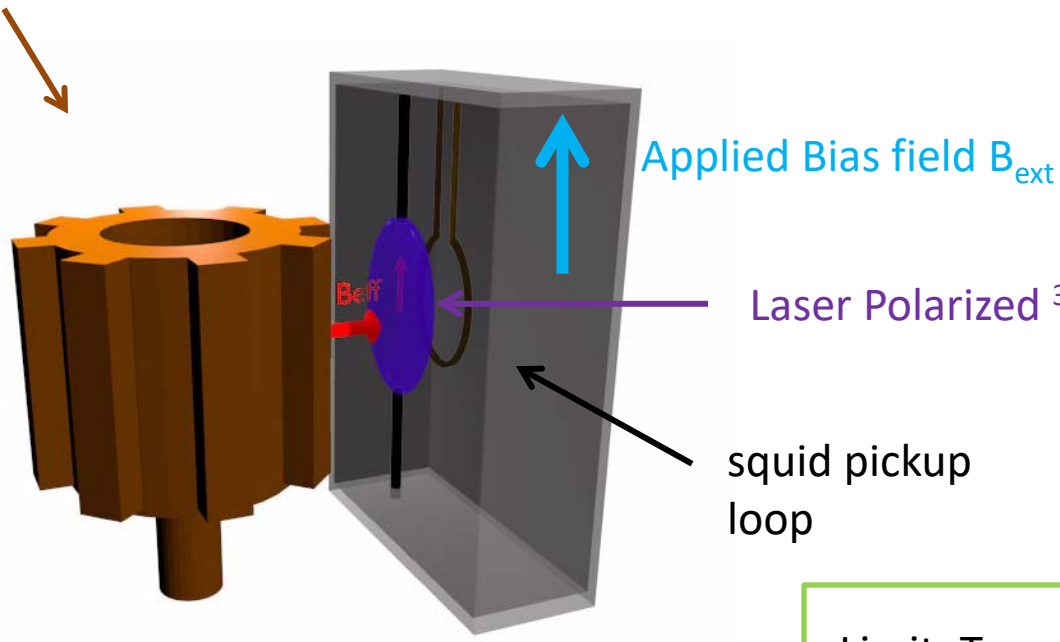
Time varying Axion B_{eff} drives spin precession
→ produces transverse magnetization

Amplitude is resonantly enhanced by Q factor $\sim \omega T_2$.

Can be detected with a SQUID

Concept for ARIADNE

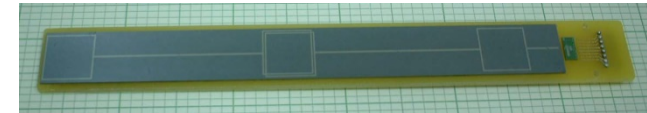
Unpolarized (tungsten) segmented cylinder sources B_{eff}



$$\omega = \frac{2\mu_N \cdot B_{\text{ext}}}{\hbar}$$

Laser Polarized ${}^3\text{He}$ gas senses B_{eff} (Indiana U)

Y.-H. Lee (KRISS)



Limit: Transverse spin projection noise

$$B_{\min} \approx p^{-1} \sqrt{\frac{2\hbar}{n_s \mu^3\text{He} \gamma V T_2}} = 10^{-20} \frac{T}{\sqrt{\text{Hz}}} \times \left(\frac{1}{p}\right) \left(\frac{1 \text{ cm}^3}{V}\right)^{1/2} \left(\frac{10^{21} \text{ cm}^{-3}}{n_s}\right)^{1/2} \left(\frac{1000 \text{ sec}}{T_2}\right)^{1/2}$$

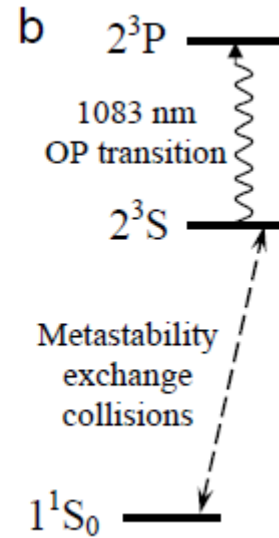
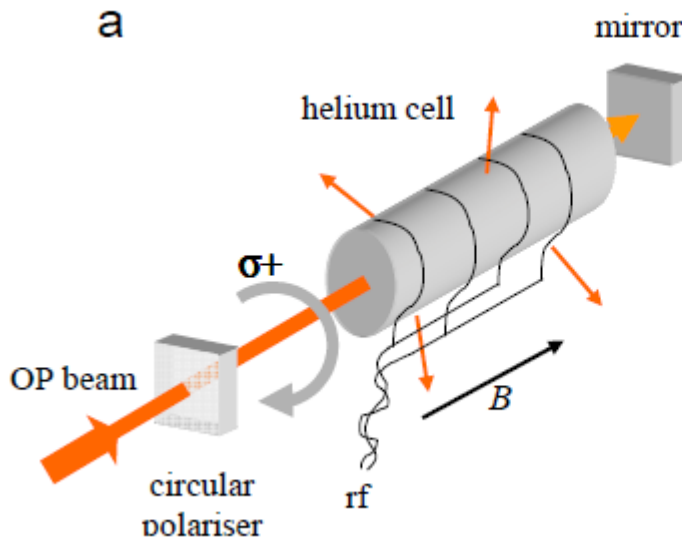
Hyperpolarized ^3He

- Ordinary magnetic fields cannot be used to reach near unity polarization

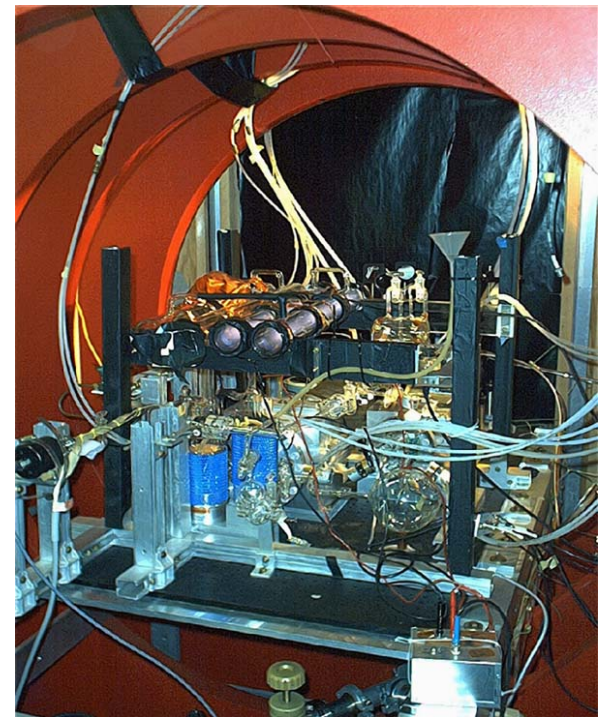
$$\exp[-\mu_N B / k_B T]$$

Optical pumping techniques

- Metastability exchange optical pumping

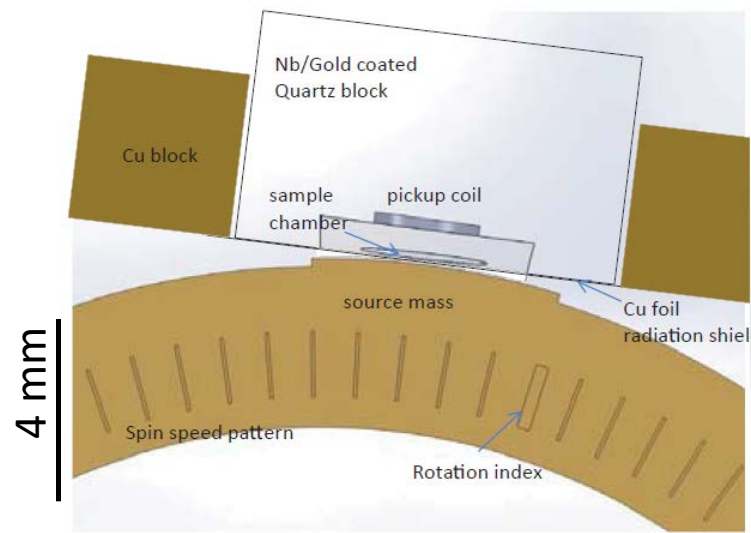
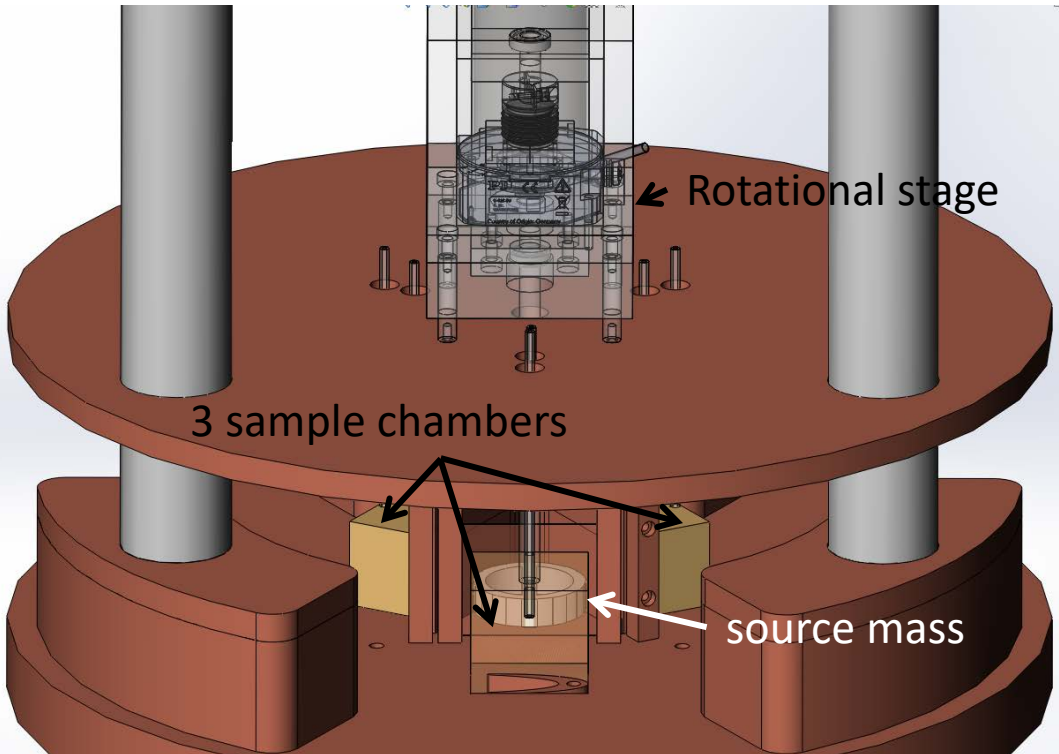


Indiana U. MEOP apparatus



Rev. Sci. Instrum. 76, 053503 (2005)

Experimental parameters



11 segments

100 Hz nuclear spin precession frequency

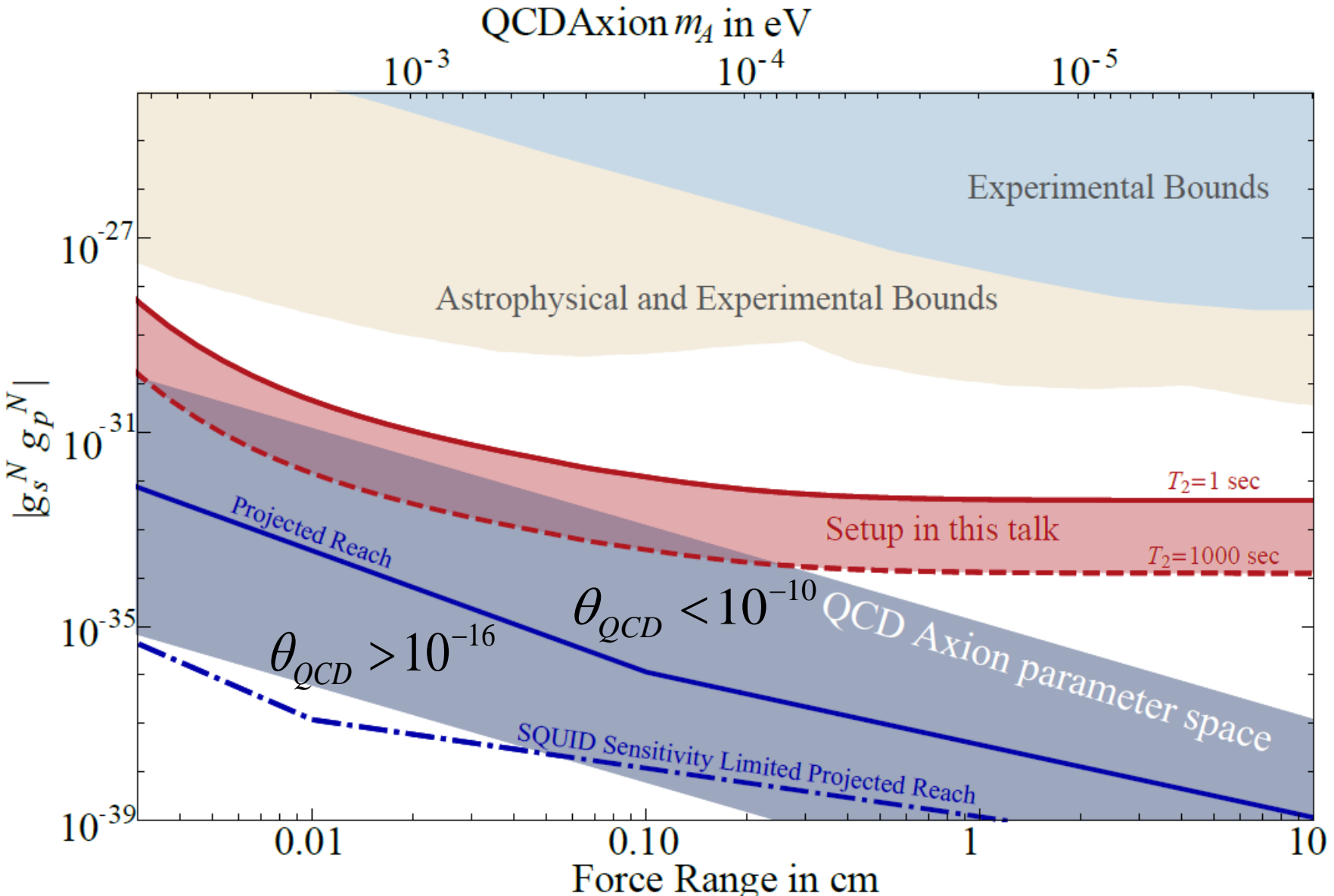
$2 \times 10^{21} / \text{cc}$ ^3He density

10 mm x 3 mm x 150 μm volume

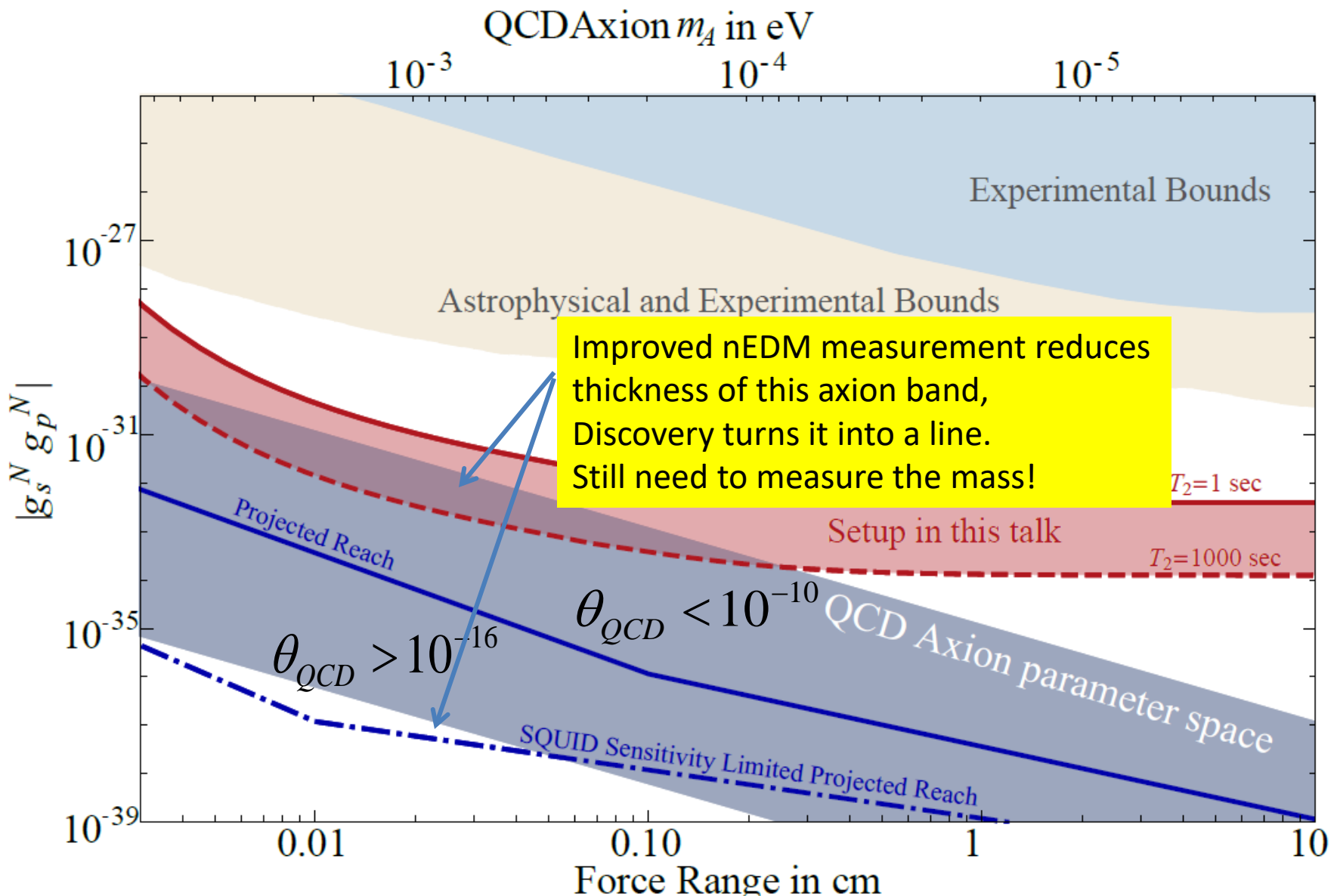
Separation 200 μm

Tungsten source mass (high nucleon density)

Sensitivity



Complementarity with nEDM experiments



Experimental challenges

Systematic Effect/Noise source	Background Level	Notes
Magnetic gradients	3×10^{-6} T/m	Limits T_2 to ~ 100 s
Vibration of mass	10^{-22} T	Possible to improve w/shield geometry
External vibrations	5×10^{-20} T/ $\sqrt{\text{Hz}}$	For $10\text{ }\mu\text{m}$ mass wobble at ω_{rot}
Patch Effect	$10^{-21} \left(\frac{V_{\text{patch}}}{0.1V} \right)^2$ T	For $1\text{ }\mu\text{m}$ sample vibration (100 Hz)
Flux noise in squid loop	2×10^{-20} T/ $\sqrt{\text{Hz}}$	Can reduce with V applied to Cu foil
Trapped flux noise in shield	7×10^{-20} $\frac{\text{T}}{\sqrt{\text{Hz}}}$	Assuming $1\mu\Phi_0/\sqrt{\text{Hz}}$
Johnson noise	$10^{-20} \left(\frac{10^8}{f} \right) \text{T}/\sqrt{\text{Hz}}$	Assuming 10 cm^{-2} flux density
Barnett Effect	$10^{-22} \left(\frac{10^8}{f} \right)$ T	f is SC shield factor (100 Hz)
Magnetic Impurities in Mass	$10^{-25} - 10^{-17} \left(\frac{\eta}{1\text{ppm}} \right) \left(\frac{10^8}{f} \right)$ T	Can be used for calibration above 10 K
Mass Magnetic Susceptibility	$10^{-22} \left(\frac{10^8}{f} \right)$ T	η is impurity fraction (see text)
		Assuming background field is 10^{-10} T
		Background field can be larger if $f > 10^8$

Table 1: Table of estimated systematic error and noise sources, as discussed in the text. The projected sensitivity of the device is $3 \times 10^{-19} \left(\frac{1000\text{s}}{T_2} \right)$ T/ $\sqrt{\text{Hz}}$

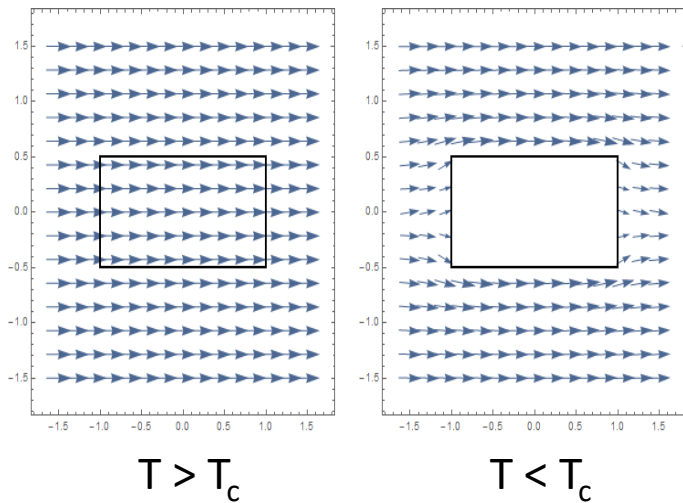
- Design/Simulation Work: Magnetic gradient reduction strategy
- Experimental testing in progress: Vibration tests, Shielding factor f test thin-film SC

Superconducting Magnetic Shielding

→ Essential to avoid Johnson noise

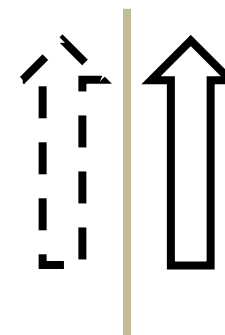
Meissner Effect

- No magnetic flux across superconducting boundary



Method of Images

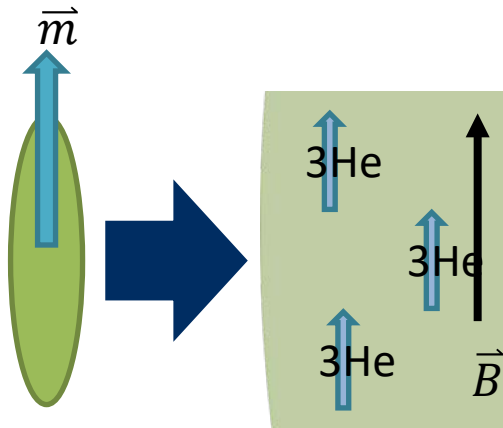
- Make “image currents” mirrored across the superconducting boundary



Dipole with image

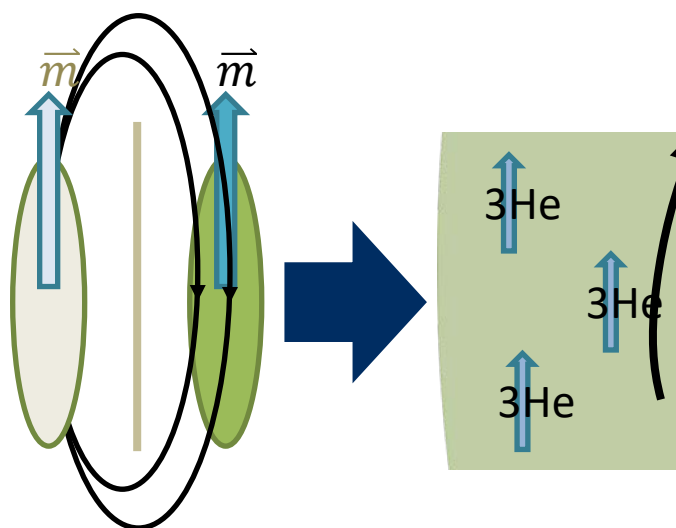
The Problem of Unwanted Images

- ARIADNE uses magnetized spheroid
 - Constant interior field



- $B_{in} = \text{const.}$
- $\frac{\vec{B}_{in}}{B_{in}} \parallel \vec{m}_i$

- Magnetic shielding introduces “image spheroid”
 - Interior field varies
- variations in nuclear Larmor frequency

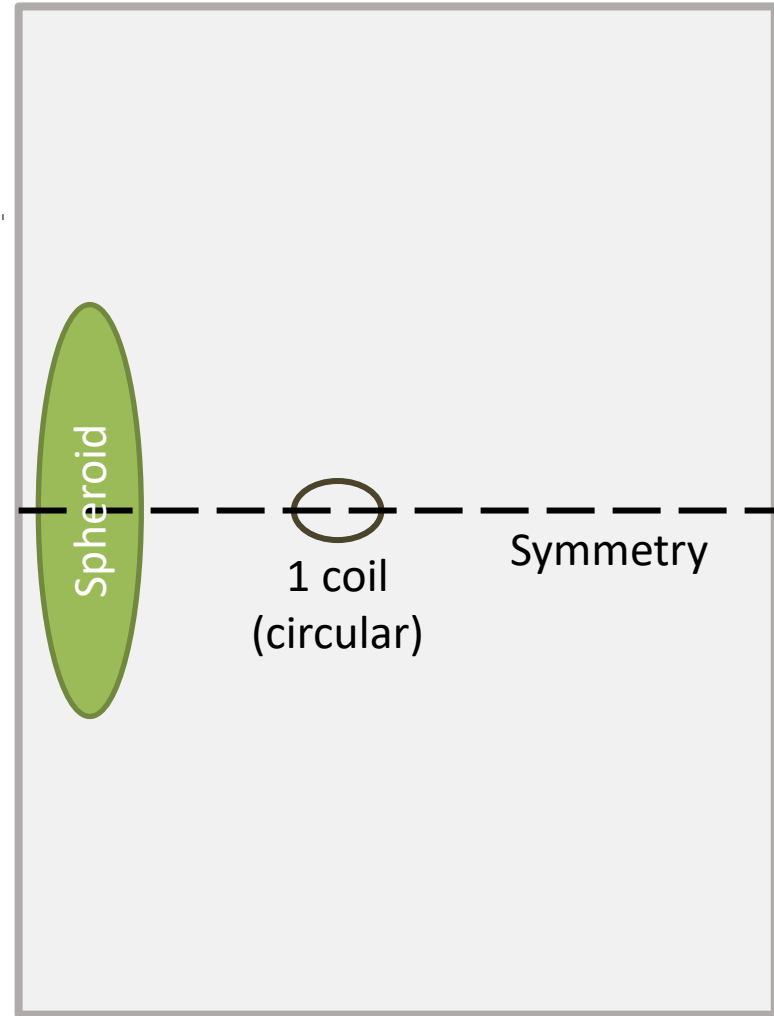


- $B_{in} \neq \text{const.}$
- $\frac{\vec{B}_{in}}{B_{in}} \nparallel \vec{m}_i$

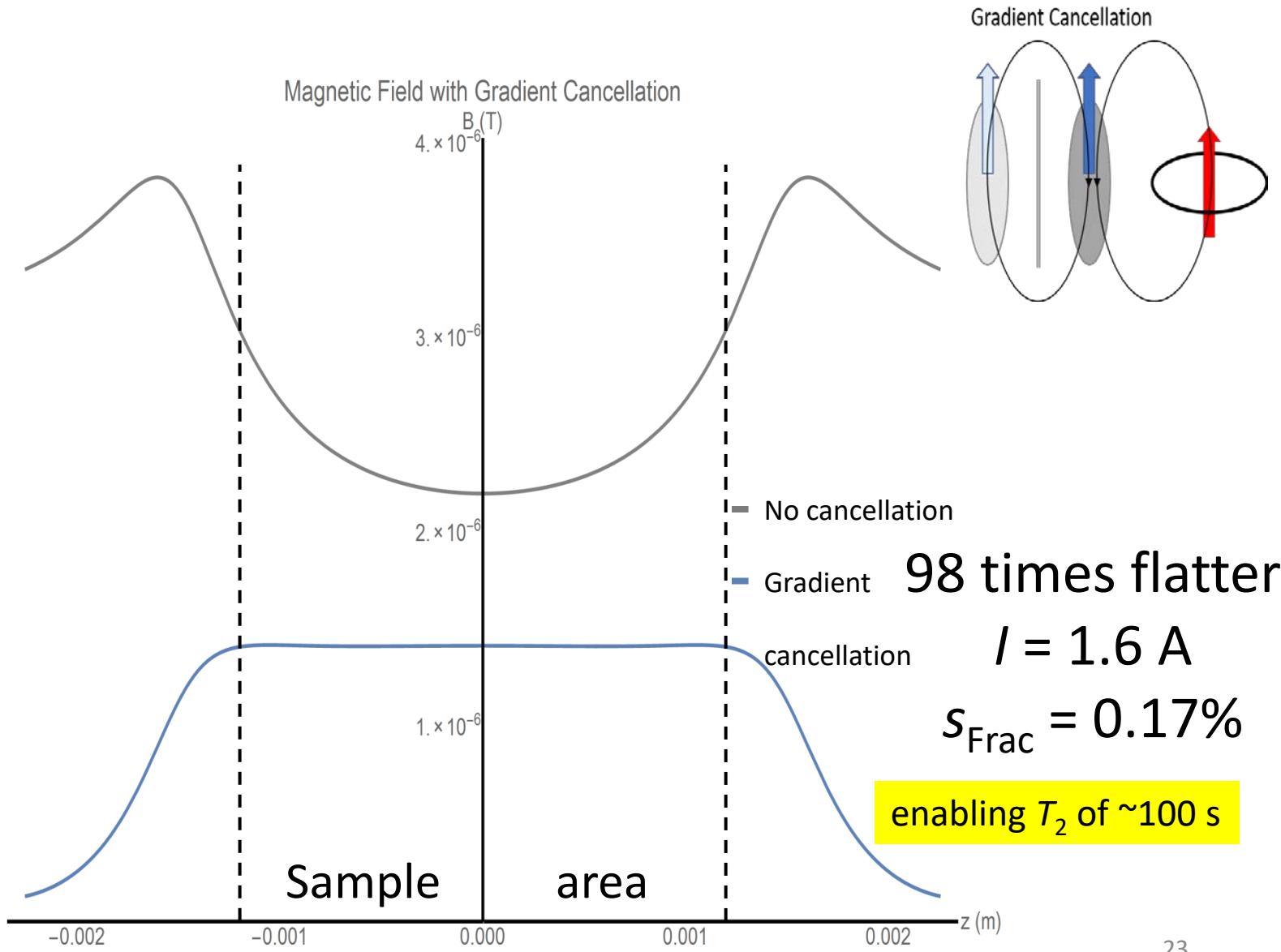
But want to drive entire sample on resonance

Flattening Solution

- 1 coil – simple configuration
- Expected field from spheroid $\sim 1 \mu\text{T}$
 - I on the 0.1 – 1 A range

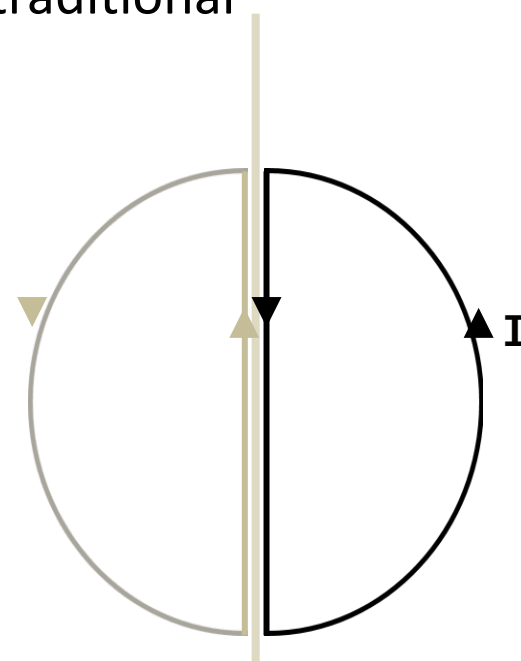


Gradient Cancellation

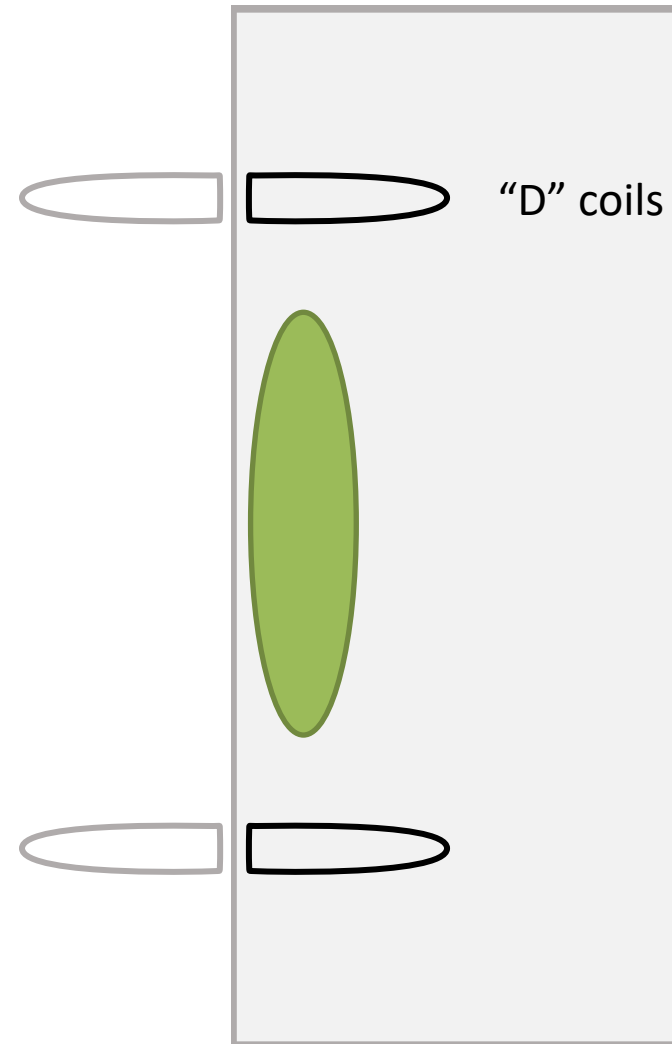


Tuning Solution – “D” Coils

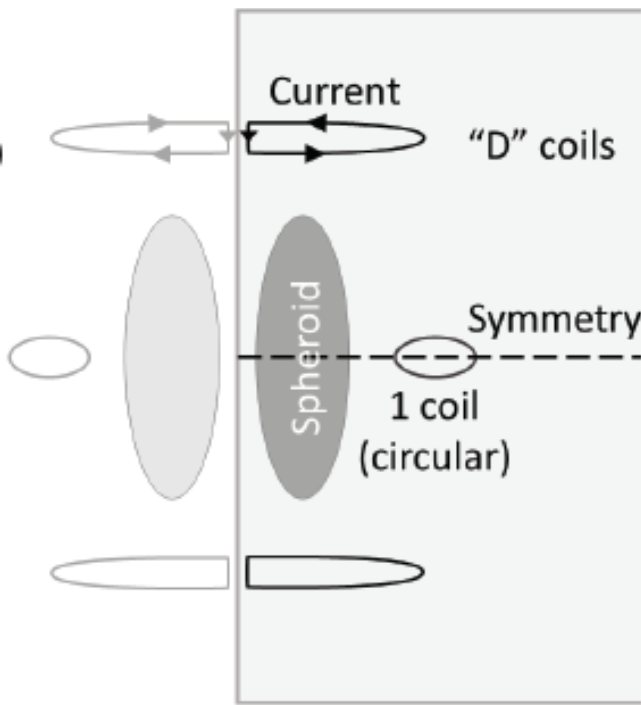
- Tune field with Helmholtz coils
 - Helmholtz field only flat near the center
 - Geometry restrictions prevent the spheroid from being centered in traditional Helmholtz coils
- “D” coils look like Helmholtz coils when their images are included
- Inner straight-line currents cancel
- Outer currents do not



One “D” coil and image (bird’s eye view)



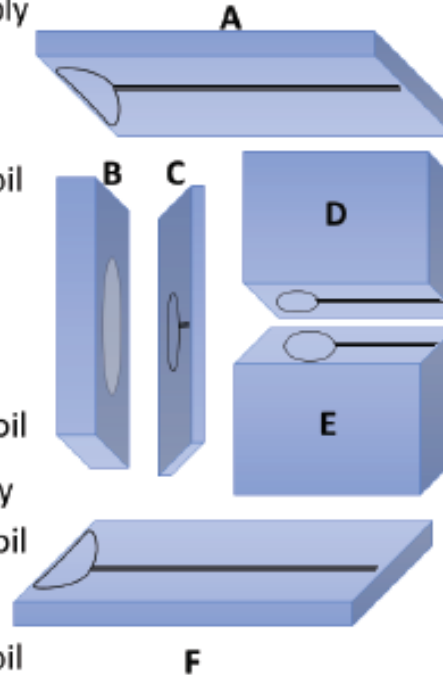
Quartz block assembly



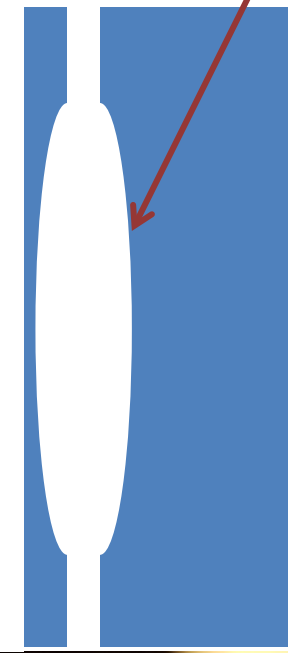
Block Assembly

Key:

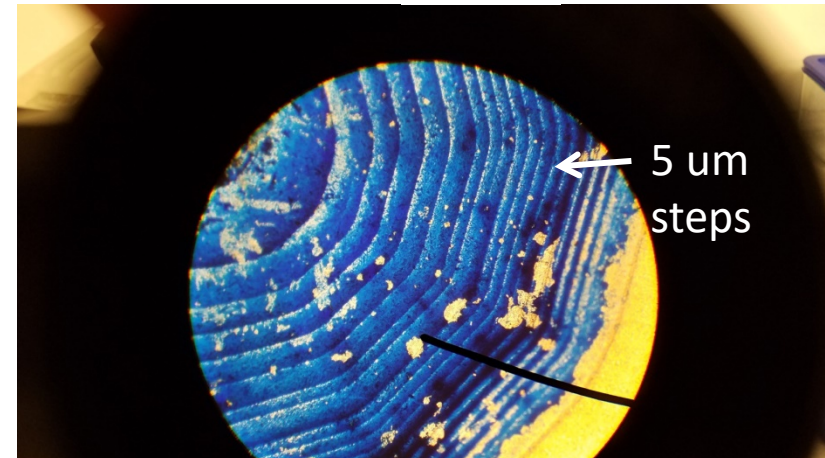
- A – Upper Helmholtz Coil
- B – Spheroid
- C – SQUID
- D – Primary Correction Coil
- E – Secondary Correction Coil
- F – Lower Helmholtz Coil



Spheriodal pocket



Milled spheriodal pocket in quartz

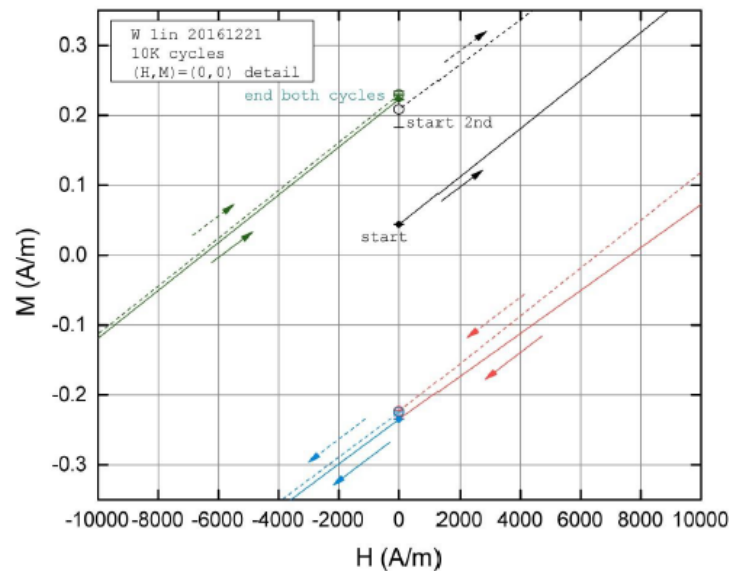
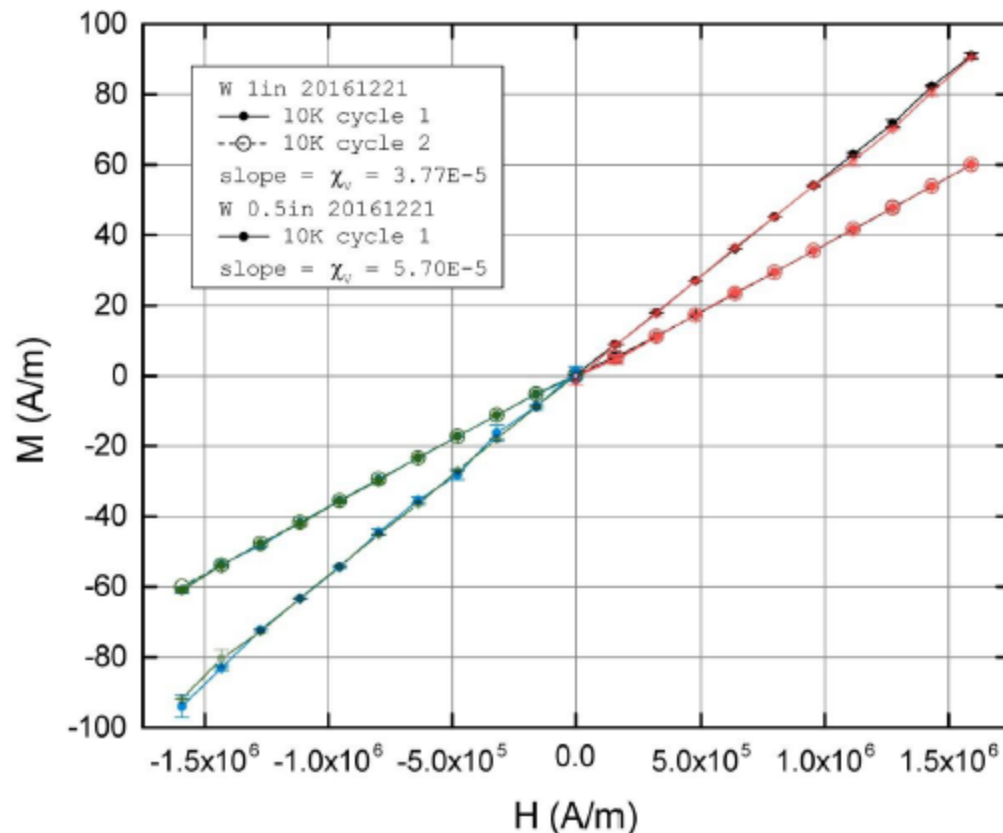


Fabrication/polishing tests is process – Aug 2017

Tungsten Source Mass Prototype

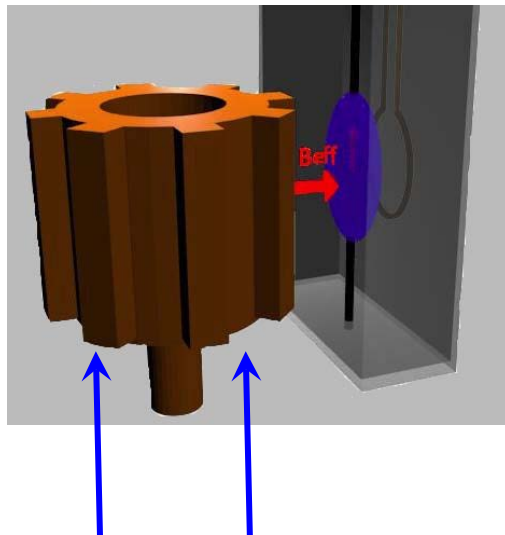
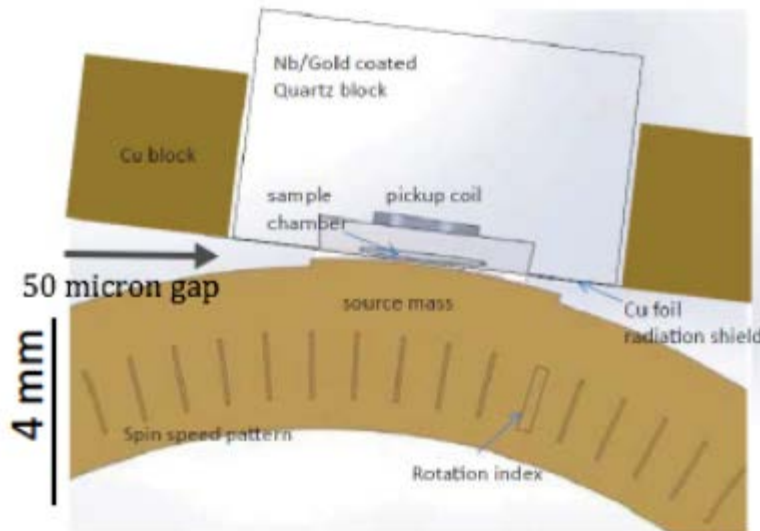
11 segments, 3.8 cm diameter Tungsten
Sprocket prototype, Wire EDM

Magnetic impurity testing in machined Tungsten
using commercial SQUID magnetometer -- Indiana

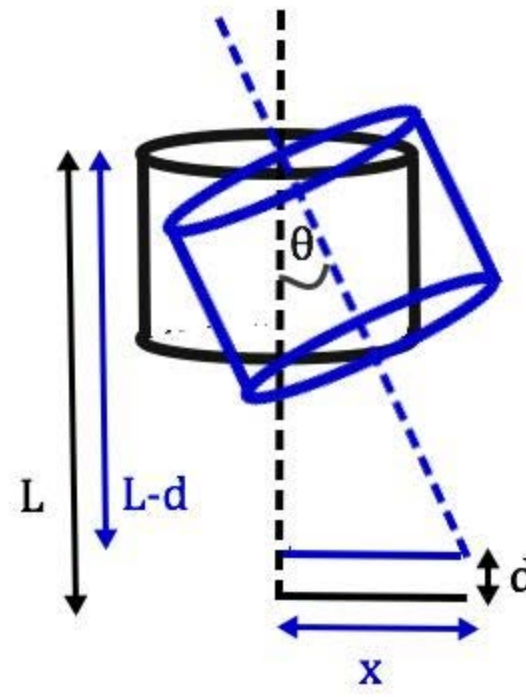


Magnetic impurities below 0.4 ppm

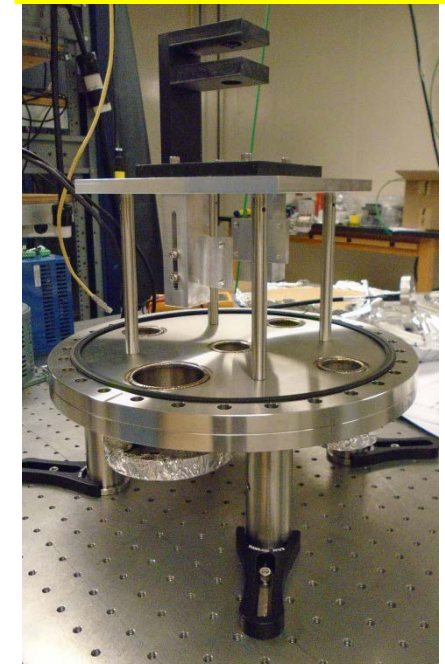
Rotary stage vibration and tilt



Interferometers

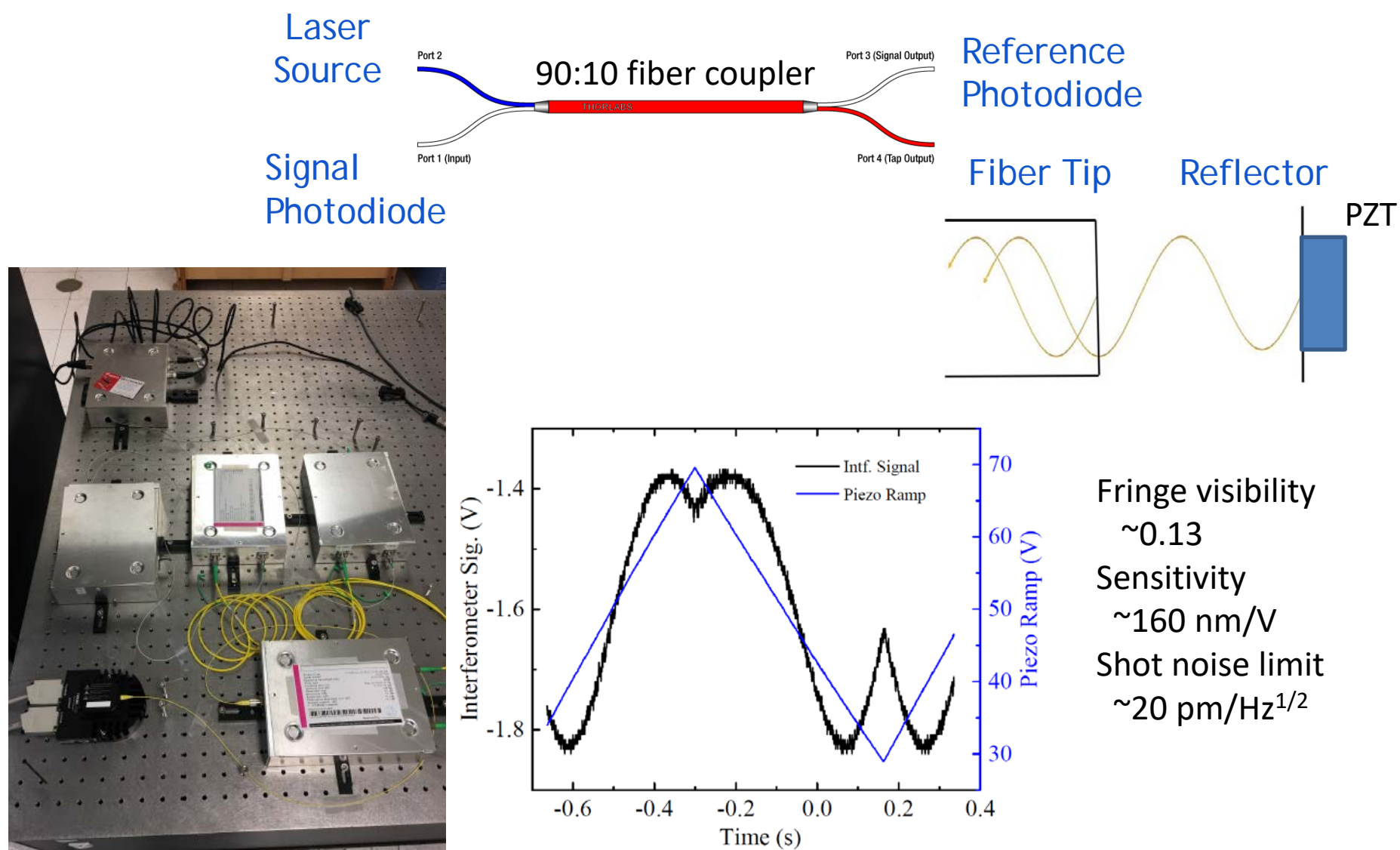


Rotary test chamber



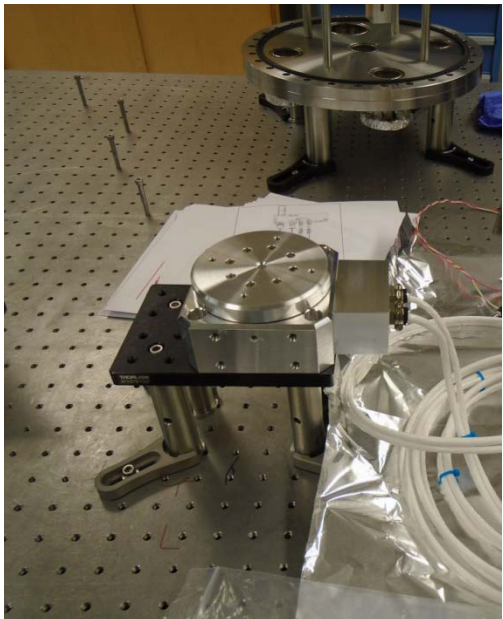
- Build an interferometer to measure the change in distance (d).
- We can find theta (Θ) from:
$$\Theta = \cos^{-1}((L-d)/L)$$
- We can solve for the wobble distance (X) by:
$$X = L\sin(\Theta)$$

Fiber-coupled laser interferometers

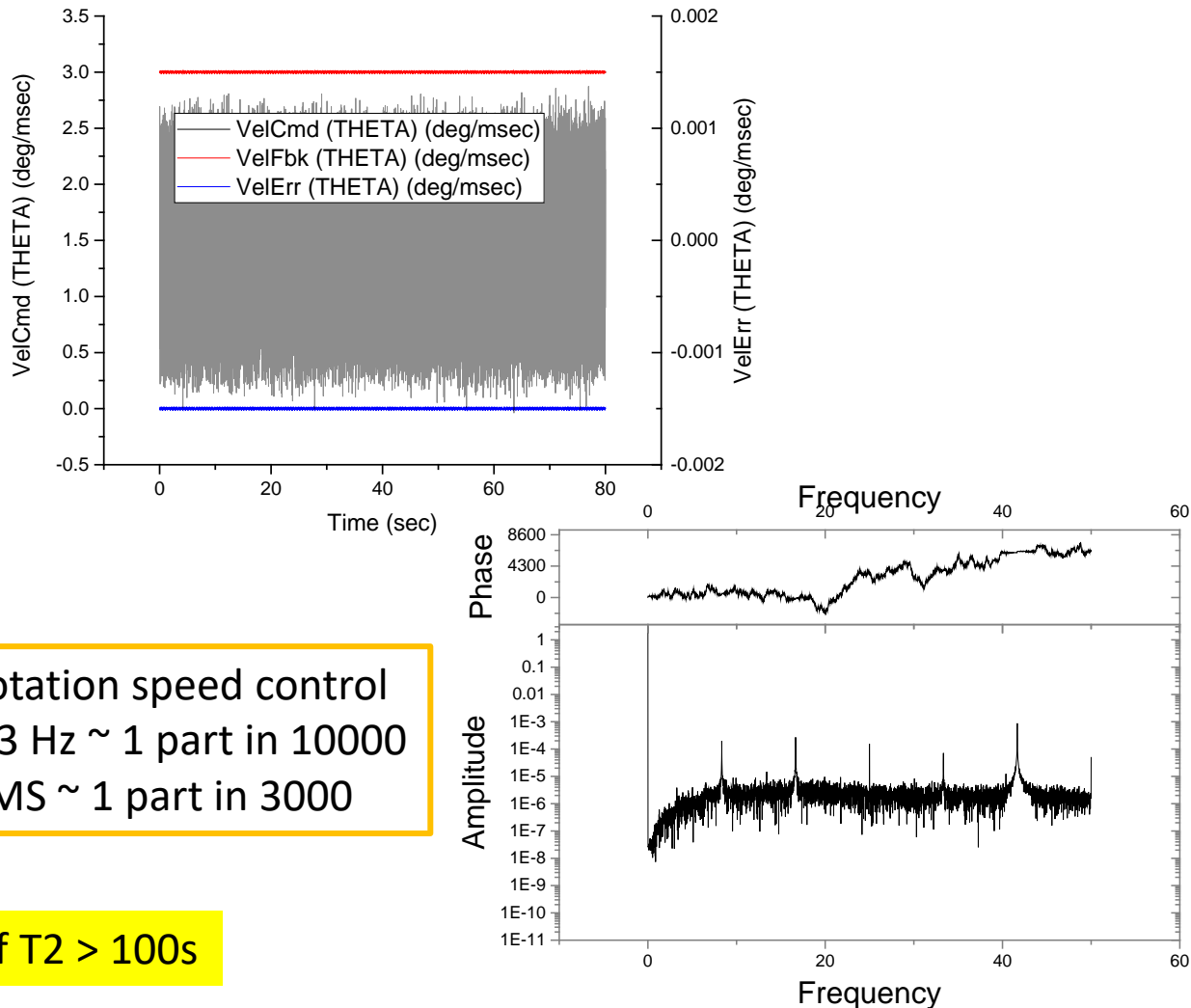


Speed stability test - direct drive stage

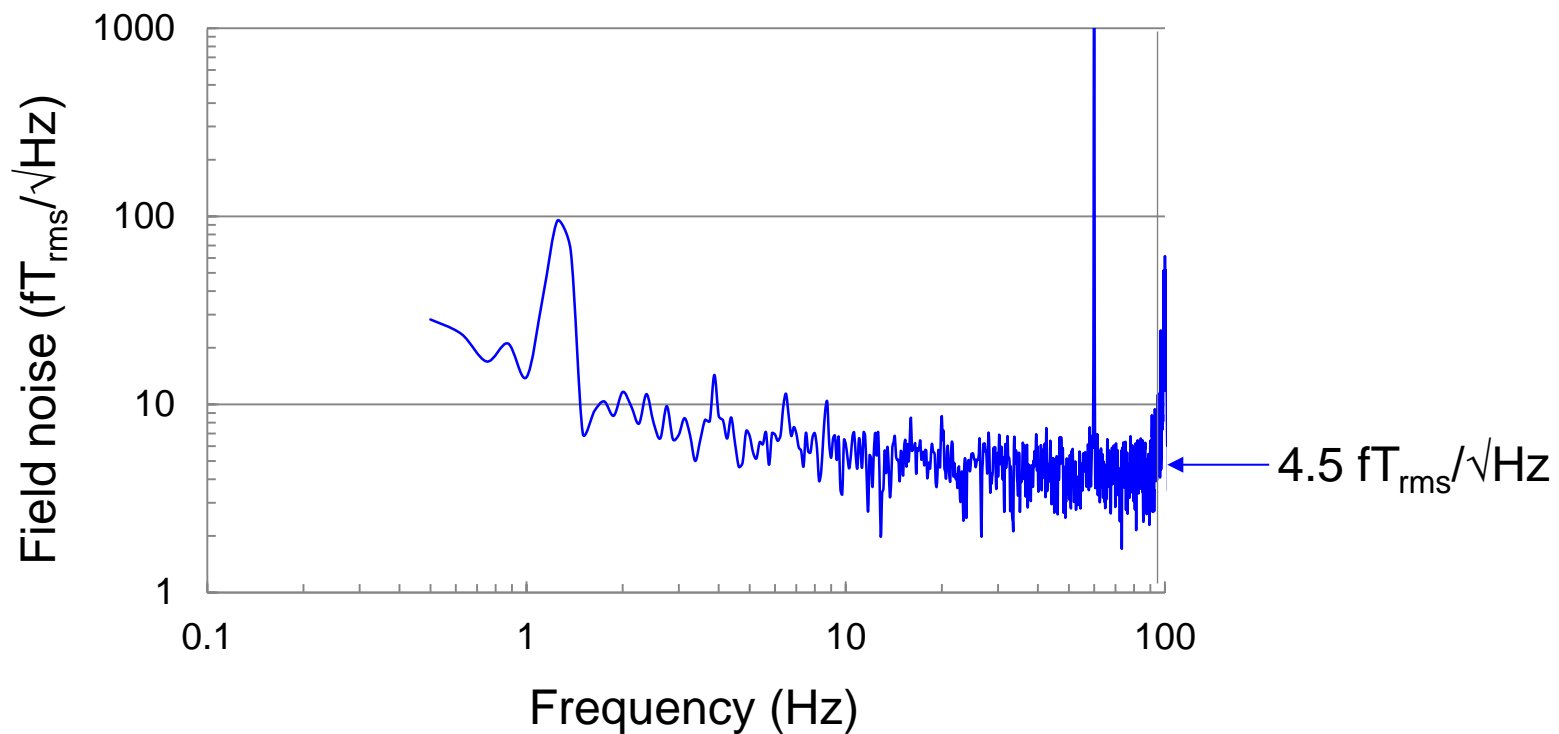
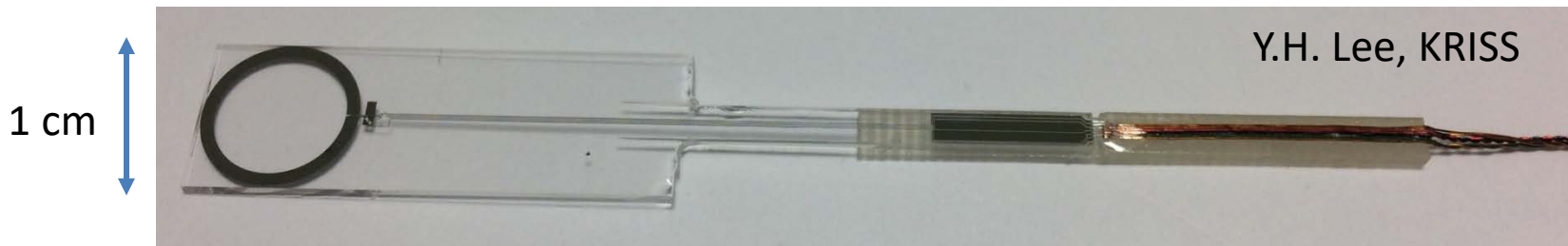
- Optical encoder
- Current feedback control



Stage speed stability error – unloaded, in air



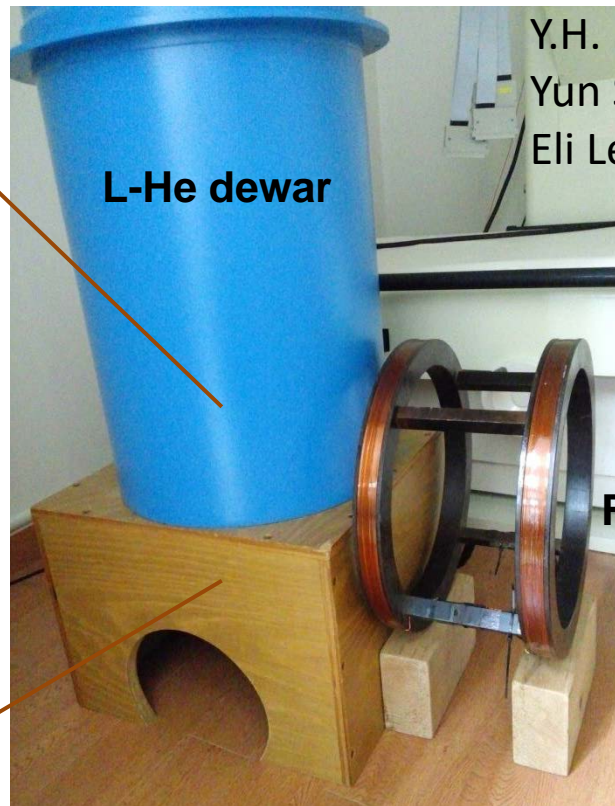
SQUID Magnetometers



Measured inside a magnetically shielded room (without Nb tube)

Preliminary test of superconductive shielding

Nb tube:
23 mm ID
1 mm thick
Length 200 mm



Y.H. Lee, KRISS,
Yun Shin (CAPP)
Eli Levenson-Falk (Stanford)

Applied field: 10-100 μT_{pp} range (at 8 Hz)

SQUID magnetometer: Near the center of Nb tube
Shielding factor: $\approx(0.5-3) \times 10^9$ for transverse field

Goal: 10^8 with thin film Nb SC shield – tests underway Summer 2017

Summary

ARIADNE → New resonant NMR method

- Gap in experimental QCD axion searches
 $0.1 \text{ meV} < m_a < 10 \text{ meV}$
- Complementary to cavity-type (e.g. ADMX) experiments
- No need to scan mass, indep. of local DM density
- Complementary to nEDM experiments
- Next tests – shielding (Stanford/Korea), vibration (UNR), ^3He system (Indiana)



Acknowledgements



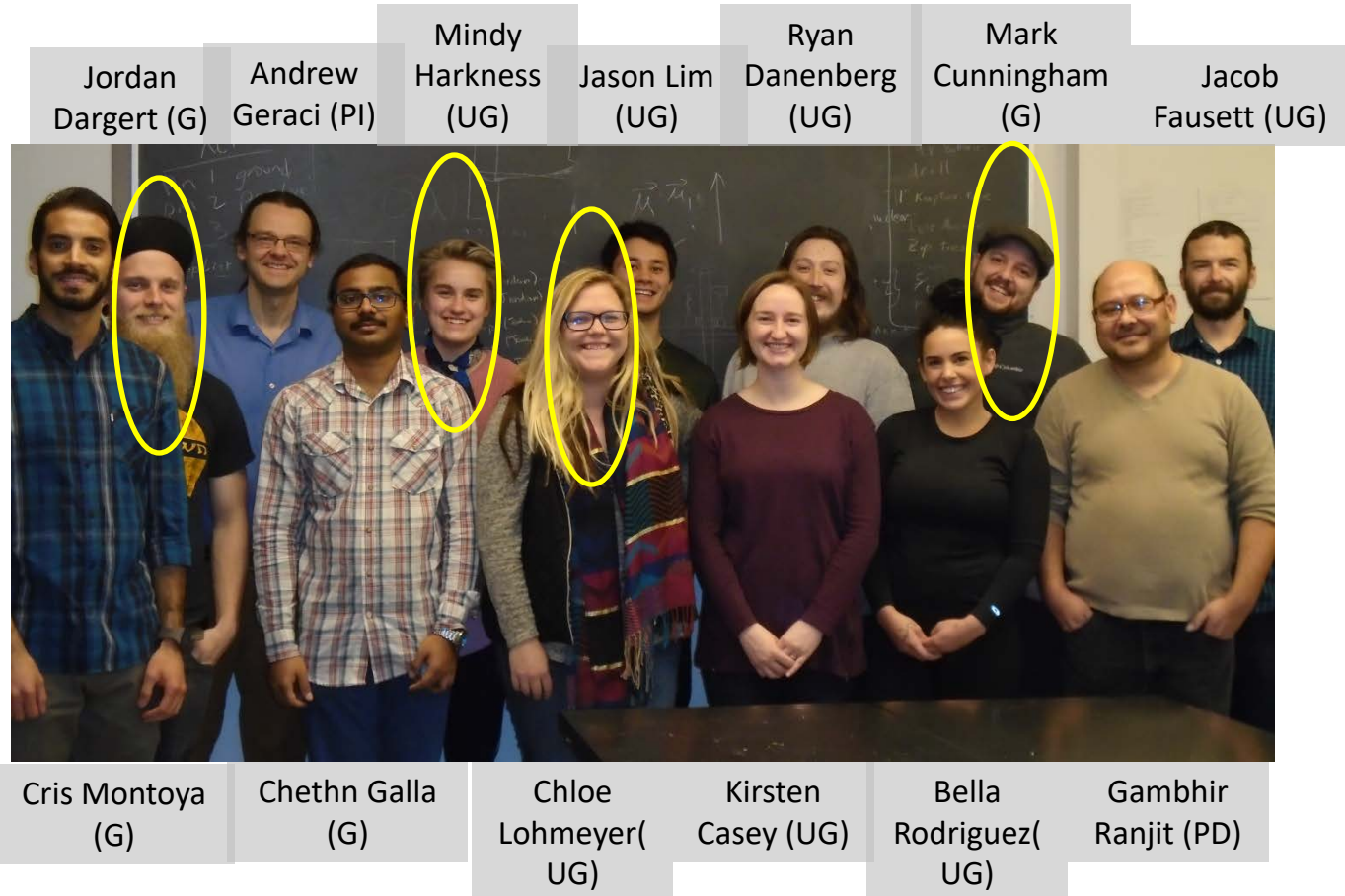
PHY-1205994

PHY-1506431

PHY-1509176

1510484, 1509176

University of Nevada, Reno



Not pictured: Apryl Witherspoon (UG),
Ohidul Mojumder (UG), Hannah Mason (UG)

Dipole-Dipole axion forces

- Spin-polarized source mass
- May be competitive with astrophysical bounds
- Magnetic shielding requirements more stringent

